King Saud University

**Arabian Journal of Chemistry**

www.ksu.edu.sa
www.sciencedirect.com

## ORIGINAL ARTICLE

# Thermodynamic study of Iron (III) removing by the synthesized α-Alumina powder and evaluating the corresponding adsorption isotherm models using Response Surface Method

**Mostafa Rajabzadeh [a], Hossein Aghaie [a],\*, Hamed Bahrami [b]**

[a] Department of Chemistry, Science and Research Branch, Islamic Azad University, Tehran, Iran
[b] Department of Chemistry, University of Zanjan, Zanjan, Iran

**Abstract** In this study, α-Alumina as an adsorbent was initially synthesized by combustion method and characterized by scanning electron microscope (SEM), transmission electron microscopy (TEM), X-ray diffraction (XRD), EDAX and Brunauer–Emmett–Teller (BET) techniques. Then the efficiency of the synthetized adsorbent for iron (III) removal was investigated and the effect of corresponding parameters such as adsorbent dose, contact time, initial concentration, temperature and solution pH on the adsorption capacity were examined and the optimums values of these parameters were concluded upon the surfaces response method. By using response surface methodology (RSM), the adsorption experimental design was performed and the statistical analysis showed that the quadratic model as well as the model terms were significant. In addition, the experimental results were examined with some suitable models, such as Langmuir, Freundlich isotherm models, where Freundlich model fitted better our experimental results. Finally, the thermodynamic behavior of the studied adsorption process was considered and the thermodynamic functions of the process were evaluated. The results showed that the Fe (III) ion adsorption onto the synthesized adsorbent is exothermic and spontaneous at the experimental conditions.

\* Corresponding author.
E-mail addresses: m.rajabzadeh89@yahoo.com (M. Rajabzadeh), hn_aghaie@yahoo.com, h.aghaie@srbiau.ac.ir (H. Aghaie), hbahrami@znu.ac.ir (H. Bahrami).
Peer review under responsibility of King Saud University.

Production and hosting by Elsevier

## 1. Introduction

Self-propagating high-temperature synthesis (SHS) or combustion synthesis (CS) is a low-cost method and effective for synthesis of various materials. Today, alumina (aluminum oxide) is used as a catalyst, adsorbent and abrasive in various industries (Lide, 2004). In this study, Aluminum oxide nanocrystal powder ($Al_2O_3$) was prepared by combustion synthesis method

using urea and glycine as fuel (Piticescu et al., 2001). Combustion synthesis is particularly a simple, safe and rapid fabrication process with energy and time savings (Edrissi and Norouzbeigi, 2007). As, many industries are rapidly expanding, so demand for metals is also rapidly rising, but high-grade ore deposits are gradually declining. Hence, the need for alternative sources of heavy metals is notably felt. Due to the presence of heavy metals in the wastes and their toxicity, the recovery of these wastes, in addition to their economic importance in preventing the reduction of natural resources, reduces also their environmental impacts (Jadhav and Hocheng, 2012). So a lot of research has been done to retrieve these compounds from the wastes, and it is currently underway. Therefore different methods such as direct magnetic separation, hydrometallogy, pyrometallogy, selective leaching and adsorption process have been used for separating the components from the wastes (Deady et al., 2016a). Red mud as a waste of the Bayer process is one of the high sources of iron in the common industry, which by using appropriate methods can be a significant source of iron extraction and prevent many environmental damages. The amount of annual bauxite waste is estimated at around 150 million tons (Deady et al., 2016b) that along with over 12 million tons of iron will be released as waste (Klauber et al., 2011). Also, some other elements such as scandium, lanthanides and rare elements are found in red mud, so red mud is the main source for retrieving these elements. Therefore the application of the effective methods for extracting these metals plays a major role in the recycling of these metals (Wang et al., 2010). For every tonne of alumina produced, 1–1.5 tonnes of red mud is generated as a waste (Kumar et al., 2006). On average, the amount of $TiO_2$, $Al_2O_3$ and $Fe_2O_3$ per 1,000,000 tons of red mud is given in Table 1.

Due to the decreasing trend of natural resources of the considered compounds as well as the high cost of them, the low cost extraction and recovery of these metals from the red mud has particular importance and it is worthwhile to mention that the red mud recovery methods have no considerable unfavorable effects on our environment. Iron (in the form of compound) is one of the important metals with a very wide variety of applications which is found in the red mud. The solubility of iron compound can be accomplished through the formation of a complex with various acids via iron reduction (Liu and Naidu, 2014). In order to examine the capability of the adsorption technique for removing Fe (III) ion from aqueous media, the effect of the sorbent dosage, the contact time, the initial concentration, the temperature and the solution pH on the removal percentage of Fe (III) ion onto the synthesized adsorbent were evaluated by using the central composite design (CCD) (see Figs. 1 and 2).

## 2. Material and method

### 2.1. Chemicals and instruments

**Chemicals:** $Al(NO_3)_3 \cdot H_2O$, $C_2H_5NO_2$ and Fe (III) nitrate were purchased from Merck Company and were used without further purification. Ammonia %65 was from Merck Company and was diluted with desired distilled water. The other necessary compounds were also taken from Merck Company.

**Instruments:** Atomic absorption set was used to determine the amount of Fe (III) ions in the remaining solution after filtering. In addition SEM, TEM, XRD, EDAX and BET/BJH

**Table 1** The amounts of some oxides that maybe available in 1000000 tons of red mud.

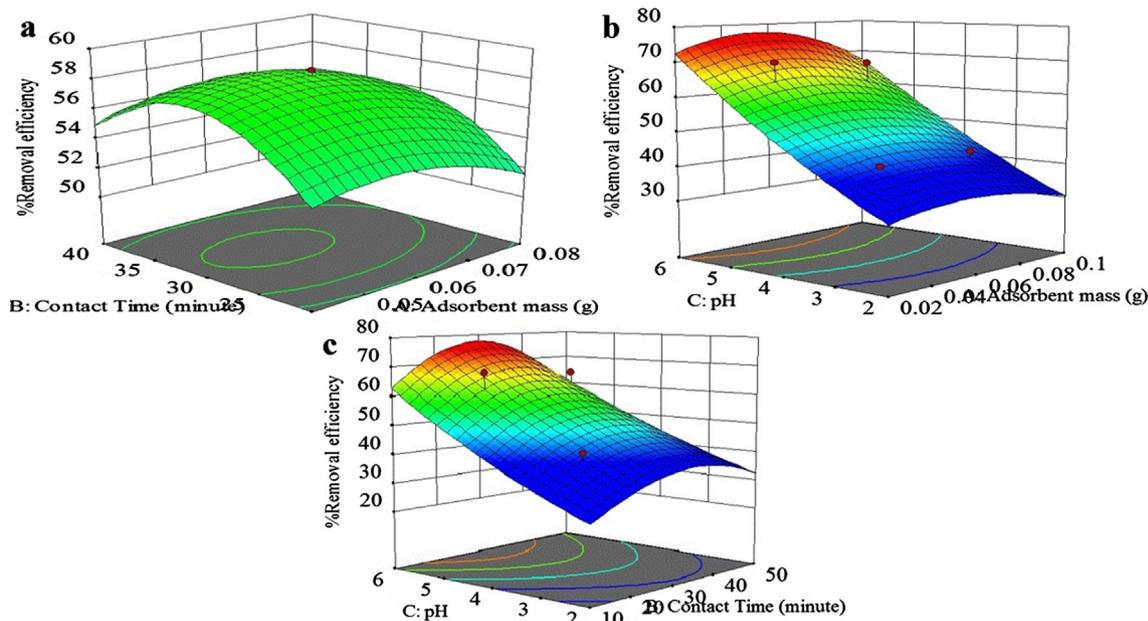| Mass of red muds (ton) | $TiO_2$ mass (ton) | $Al_2O_3$ mass (ton) | $Fe_2O_3$ mass (ton) |
|---|---|---|---|
| 1,000,000 | 74,800 | 188,700 | 236,000 |



**Fig. 1** Fe (III) ions removal percent as a function of (a) adsorbent dosage and contact time, (b) adsorbent dosage and pH, (c) pH and contact time.
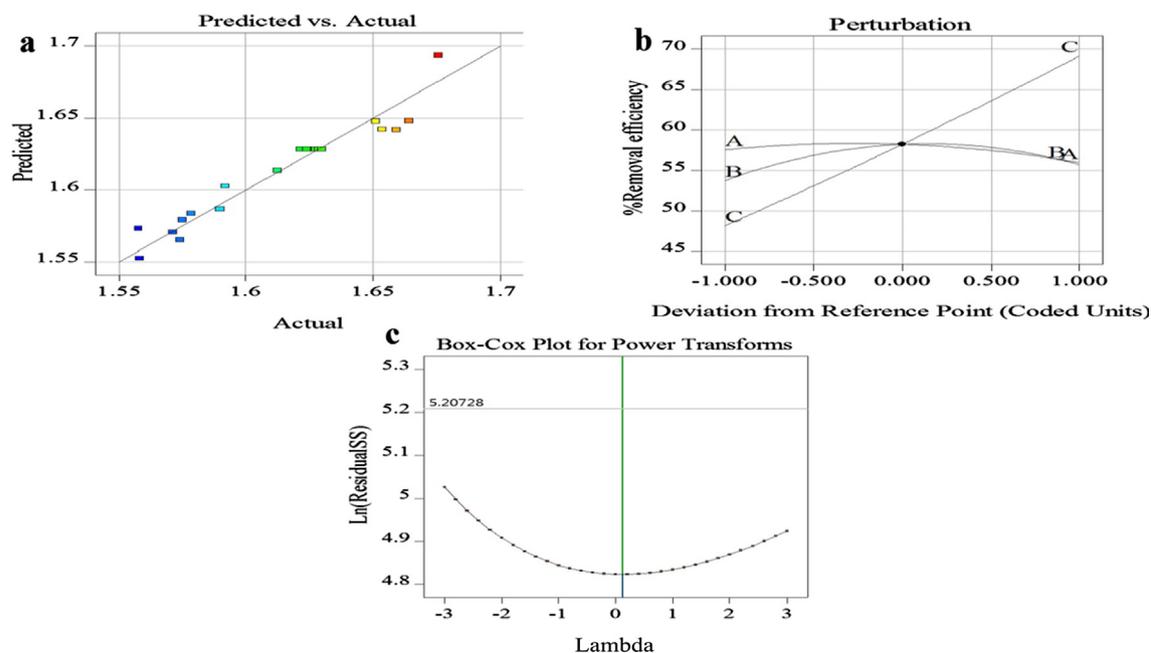
**Fig. 2** (a) Plot of standard residuals versus predicted values, (b) Perturbation diagram to compare the effect of A, B and C on the removal percentage, (c) cox box plot.

sets were used for the synthesized α-Alumina powder characterization (see Fig. 3).

Due to its porous structure, α-Alumina can be used as an appropriate adsorbent in industry. So, aluminum nitrate deca hydrate was used to produce α-Alumina according to the following reaction (Al'myasheva et al., 2005). In this step, the necessary reagents according to the reaction formula were dissolved in a sufficient distilled water and the products of the reaction were dried and then heated in a heating furnace near to 350 °C for half hours (Pati et al., 2000).

$$2Al(NO_3)_3(aq) + 4C_2H_5NO_2(aq) + 3NH_4NO_3(aq) \rightarrow Al_2O_3(s) + 8CO_2(g) + 16H_2O(g) + 8N_2(g) \quad (1)$$
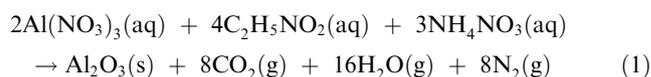
The obtained alumina at this step is not so efficient as an adsorbent, so, for activating it and eliminating the probable hydrocarbon in the obtained product, it was heated up to
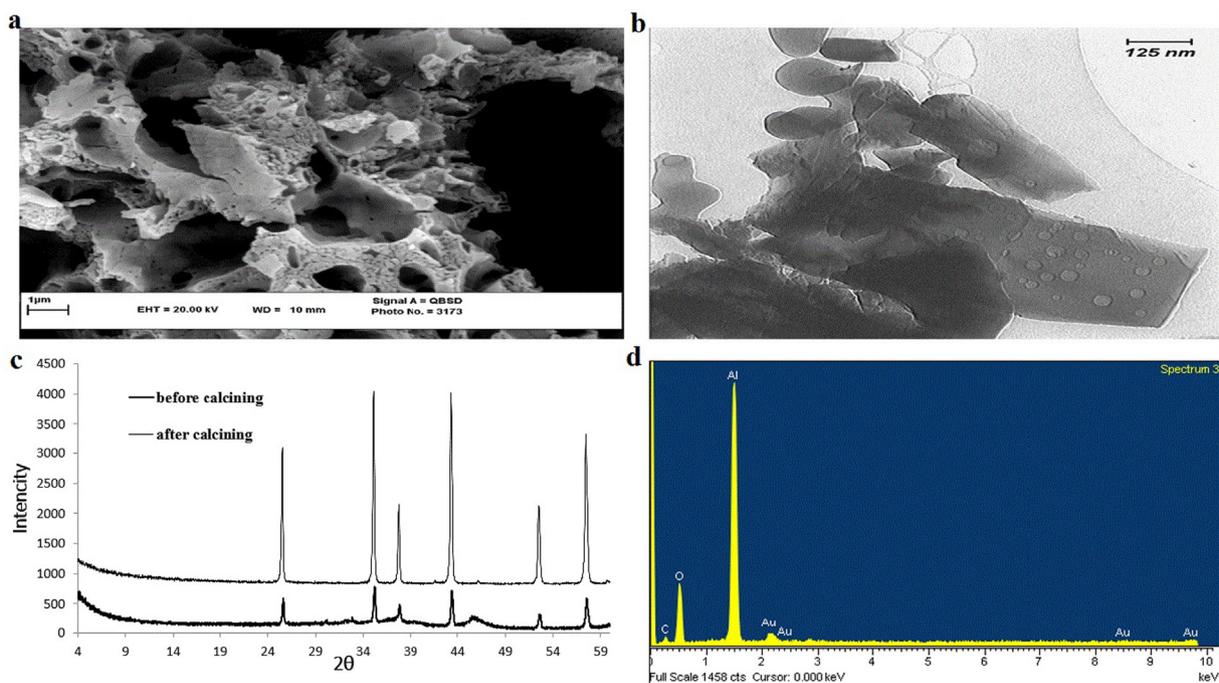


**Fig. 3** (a) SEM image, (b) TEM image, (c) XRD spectrum, (d) EDAX spectrum of the synthesized α-Alumina.

1200 °C for 2 h in order to reach the fairly pure crystalline powder of α-Alumina that can be used as an effective sorbent (Wen et al., 1999).

## 2.2. Designing a typical adsorption experiment

In this study, the procedure of carrying out a typical adsorption experiment was as follow: A sample of Fe (III) solution with a known concentration (15.0 mg/L respect to Fe (III) ion) was prepared from the stock solution (1000 mg/L). Then 0.060 g of the prepared α-Alumina (the optimum dosage) was added to it. The value of pH was adjusted at 5.0 (the optimum pH) and temperature at 25 °C (the optimum temperature). Then the mixture was stirred normally for 30 min under the above conditions for reaching to the equilibrium state. Then, the mixture was filtered and the concentration of Fe (III) in the ultimate solution was determined by atomic absorption. In addition, the initial concentration ($C_0$) of Fe (III) ion in the test solution was also determined by the same instrument and used for the following computation:

$$\text{Adsorption percentage (Ad\%) } \% = \frac{C_0 - C_e}{C_0} * 100 \quad (2)$$

where $C_0$ and $C_e$ are the initial and equilibrium concentrations of Fe (III) ion in the test solution.

## 2.3. Adsorption experiments and the response surface method

In order to save time and expenses, the design of the response surface method was used along with the experimental data to model the adsorption process. Therefore the experimental design method was used to evaluate the synthesized α-Alumina efficiency for Fe (III) ions adsorption. The Design of Experiments (DOE) is a powerful method, first developed by Ronald Fisher in the 1920s to study the simultaneous effects of several factors on a given response (Montgomery et al., 2012). In order to use this method, at first, in each run, a solution of Fe (III) ions with a concentration close to the actual sample (Fe (III) ion in red mud) was prepared and a suitable amount of the synthesized α-Alumina was added to it and then the obtained mixture was agitated on a shaker at 150 rpm at room temperature and finally was used to optimize the adsorption conditions. Here, twenty experiments including 6 repeated runs at the central point were carried out. Design Expert Version 11 was used to generate the Central Composite Design (CCD) experiments, and optimize the levels of the independent variables, and evaluated interactions of the process parameters, while the removal percentage of Fe (III) ions was taken as the dependent variable. In this study, the various factors such as the initial concentration, the contact time, the adsorption dosage, the temperature and pH were considered as the effective parameters of the adsorption process, based on the

RMS method at 25 °C and 150 rpm, while the Fe removal efficiency (Y) was selected as the response function. These parameters and their variation ranges were evaluate in 5 levels (−2, −1, 0, +1, +2), as shown in Table 2.

For the statistical regression and graphical analysis of the obtained data, the Design Expert software was used and the removal efficiencies indicating the measure of the interaction between dependent and independent variables were evaluated by the following quadratic polynomial equation (an equation of second degree):

$$\%Y = +1.63 - 0.0027A + 0.0034B + 0.0352C$$
$$+ 0.0002AB - 0.0003AC - 0.0034BC - 0.0050A^2$$
$$- 0.0121B^2 - 0.0013C^2 \quad (3)$$

where A, B and C represent the adsorbent dosage, the contact time and pH respectively. The design expert version 11 was performed, in order to evaluate the optimal conditions of the studied process. The result of using the experiments design for the present study is gathered in Table 3 and Figs. 1 and 2.

Moreover analysis of variance (ANOVA) was used for statistical analysis. Indeed ANOVA is a collection of the statistical models along with their associated estimation procedures (such as the "variation" among and between groups) that can be used to analyze the differences among the group means in a sample. In the contrary of the usefulness of the model, it is quite necessary to evaluate the statistical adequacy and the significance of the model (Segurola et al., 1999). If the F-value of the model being near 16.88 implies the model is significant but there is only a 0.01% chance that an F-value so large could occur due to the noise. To evaluate the model presented here and to assess the statistical adequacy of the results, the normal probability charts and the Cox Box should be used (Fig. 2). According to the empirical results, the form of the presented models in the applied concentration range are sufficiently reliable and have sufficient accuracy in predicting the Fe (III) ion adsorption onto the synthesized adsorbent. Also, the predicted correlation coefficient, which is considered as a measure of the data deviation from those provided by the model, can also be used as a criterion for the considered evaluations. In turn the p-value or probability value or asymptotic significance of the model is the probability for a given statistical model, when the null hypothesis is true and the statistical summary (such as the mean sample difference between two compared groups) would be greater than or equal to the actual observed results (Wasserstein and Lazar, 2016) (Table 4). In Table 4, the F-value is the test for comparing the source's mean square to the residual mean square, also the mean square shows the sum of the squares divided by the degrees of the freedom. The residual row shows how much variation in the response is still unexplained, the Lack of Fit is the amount of the model predictions miss of the observations, the pure error is the amount of the difference between replicate runs and the cor

**Table 2** Central composite design.

| Name | Units | Low | High | −alpha | + alpha |
|---|---|---|---|---|---|
| Adsorbent mass | g | 0.04 | 0.08 | 0.02 | 0.1 |
| Contact Time | minute | 15 | 35 | 10 | 40 |
| pH | mol/L | 3 | 5 | 2 | 6 |

**Table 3** The results of using the experiments design.

| Run | Factor 1 A:Adsorbent mass (g) | Factor 2 B: Contact Time (minute) | Factor 3 C:pH | Response %adsorption |
|---|---|---|---|---|
| 1 | 0.04 | 20 | 3 | 43.21 |
| 2 | 0.06 | 10 | 4 | 40.17 |
| 3 | 0.06 | 50 | 4 | 47.66 |
| 4 | 0.1 | 30 | 4 | 48.12 |
| 5 | 0.06 | 30 | 6 | 73.88 |
| 6 | 0.04 | 40 | 5 | 65.23 |
| 7 | 0.08 | 20 | 5 | 67.98 |
| 8 | 0.08 | 40 | 5 | 66.14 |
| 9 | 0.06 | 30 | 4 | 56.11 |
| 10 | 0.08 | 40 | 3 | 44.12 |
| 11 | 0.06 | 30 | 4 | 57.89 |
| 12 | 0.06 | 30 | 4 | 56.89 |
| 13 | 0.06 | 30 | 4 | 58.21 |
| 14 | 0.02 | 30 | 4 | 53.54 |
| 15 | 0.06 | 30 | 4 | 57.49 |
| 16 | 0.06 | 30 | 2 | 40.29 |
| 17 | 0.08 | 20 | 3 | 43.89 |
| 18 | 0.04 | 40 | 3 | 44.89 |
| 19 | 0.04 | 20 | 5 | 69.78 |
| 20 | 0.06 | 30 | 4 | 58.61 |

**Table 4** Analysis of variance (ANOVA) for response surface quadratic model.

| Source | Sum of Squares | $d_f$ | Mean Square | F-value | p-value | |
|---|---|---|---|---|---|---|
| **Model** | 1910.01 | 9 | 212.22 | 16.88 | < 0.0001 | Significant |
| A-Adsorbent mass | 8.73 | 1 | 8.73 | 0.6944 | 0.4241 | |
| B- Contact Time | 6.89 | 1 | 6.89 | 0.5479 | 0.4762 | |
| C-pH | 1604.00 | 1 | 1604.00 | 127.55 | < 0.0001 | |
| AB | 0.1984 | 1 | 0.1984 | 0.0158 | 0.9025 | |
| AC | 0.0800 | 1 | 0.0800 | 0.0064 | 0.9380 | |
| BC | 8.61 | 1 | 8.61 | 0.6848 | 0.4273 | |
| $A^2$ | 47.50 | 1 | 47.50 | 3.78 | 0.0806 | |
| $B^2$ | 242.14 | 1 | 242.14 | 19.25 | 0.0014 | |
| $C^2$ | 0.9001 | 1 | 0.9001 | 0.0716 | 0.7945 | |
| **Residual** | 125.75 | 10 | 12.58 | | | |
| Lack of Fit | 121.57 | 5 | 24.31 | 29.04 | 0.0011 | Significant |
| Pure Error | 4.19 | 5 | 0.8372 | | | |
| **Cor Total** | 2035.77 | 19 | | | | |
| **$R^2$** | 0.9775 | | | | | |
| **Adjusted $R^2$** | 0.9573 | | | | | |

total shows the amount of the variation around the mean of the observations.

The perturbation pattern in Fig. 2(b) shows that all three parameters of the adsorption process such as, adsorbent dosage, contact time and pH are effective on the adsorption capacity. Indeed by increasing the adsorbent dosage up to 0.060 (g), the amount of the adsorption increases and then decreases; or as the contact time increases, the amount of adsorption also increases and reaches its maximum value at time of 30.0 min and then decreases slowly with increasing the contact time. The pH effect is more obvious than the other effects, and by increasing pH, the adsorption capacity increases. Also, The Cox-Box plot is a helpful tool for determination of the most appropriate power transformation in applying the response data (Fig. 2(c)).

## 3. Results and discussion

### 3.1. Characterization of the synthesized α-Alumina

Characterization of the synthesized α-Alumina was performed by SEM, TEM, XRD, EDAX and BET techniques (Fig. 3). The SEM and TEM images of the synthesized α-alumina are shown in Fig. 3(a) and (b) respectively. These images revealed some specific characters of the synthesized α-alumina. In Fig. 3 (c), the XRD patterns of alumina before heating it up to 1200 °C and after heating are shown (Bodaghi et al., 2009). These spectra demonstrate that the primary alumina (the form before heating) is almost amorphous, but the final form (after calcining at 1200 °C) has fairly crystalline character indicating

that it can be considered as a good sorbent for the adsorption process (He et al., 2005). The related EDAX spectrum is shown in Fig. 3(d) indicating a fairly high purity of the synthesized α-Alumina. The BET experiment of the synthesized α-Alumina revealed several features of the synthesized α-Alumina, such as:

Adsorption cross section area $= 0.162$ nm$^2$
Mean pore diameter 49.76 nm, $a_s$, BET $= 2.53$ m$^2$/g, $a_s$, Lang $= 3.10$ m$^2$/g, $\alpha_p = 3.52$ m$^2$/g.

### 3.2. The effect of adsorbent dosage

The batch study was set up to determine the effect of the α-Alumina dosage on Fe (III) ions adsorption. The dosage was varied from 0.020 mg up to 0.10 g. The respective amount of α-Alumina was added to 50 mL of Fe (III) ion solution ($C_0 = 15$ mg/L) and the respect removal percent was determined (using the experimental procedure). As shown in Fig. 4(a), by increasing the adsorbent dose, the iron (III) removal percent is initially increased and then decreased. On the basis of Fig. 4(a), we may choose the value of 0.060 g as the optimum dose. The adsorption capacity decreasing beyond the optimum dose, maybe comes from the free sites shortcoming on the sorbent surface and at the same time due to the particles agglomeration.

### 3.3. The effect of contact time

To establish the equilibrium contact time, the adsorption experiments were carried out at different contact times (from 10:0 to 40:0 min). Our results showed that the adsorption efficiency increases gradually and then fairly becomes constant with increasing the contact time (Fig. 4(b)). The reason may be that the adsorption process goes toward completion with time and finally reaches the equilibrium state. Looking the Fig. 4(b), we may conclude that 30.0 min may be fairly an optimum contact time respect to the studied adsorption.

### 3.4. The effect of pH

As shown in Fig. 4(c), by increasing pH, the Fe (III) ion removal is initially increased and then decreased slowly. In general the uptake of heavy metal ions by the suitable sorbents is strongly influenced by pH solution, since it determines the surface charge of the adsorbent and the degree of solute ionization and specificities of the adsorbate (Amuda et al., 2007). The pH solution was adjusted by adding the required amount of dilute NH$_3$ or HNO$_3$ solutions. Adjusting the pH solution on a suitable value is very important respect to the studies adsorption. At low pH, H$^+$ ions maybe contribute in competition with the adsorbing cations and this situation will be occurred for the adsorbing anions at enough high pH. At high pH, there is another very important risk, where the considered
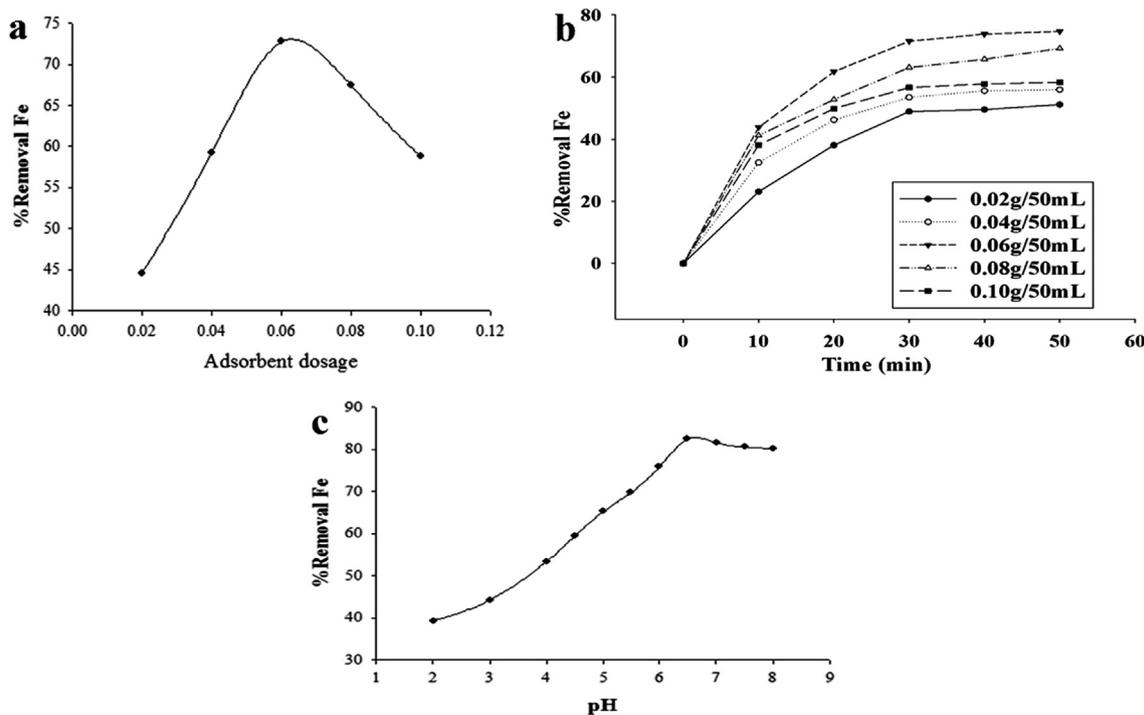


**Fig. 4** (a) The effect of the adsorbent dosage (g) on the Fe (III) ions removal percent, ($C_0 = 15$ mg/L, pH = 5, t = 25 °C, contact time = 30.0 min), (b) The effect of contact time on the removal percentage of Fe (III) ions onto the synthesized adsorbent. The selected dosages were 0.020, 0.040, 0.060, 0.080 and 0.100 g, initial concentration = 15 mg/L, pH = 5.0 and t = 25 °C. (c) The effect of pH solution on the removal percent of Fe (III) ions onto the synthesized adsorbent (initial concentration = 15 mg/L, contact time = 30.0 min, t = 25 °C, dosage mass = 0.060 g).

adsorbate cations will be precipitated as the own hydroxides which would seriously interfere in the adsorption process.

In addition the pH solution influences the distribution of the active sites on the surface of the nanostructured $Al_2O_3$ (Rahmani et al., 2010). The effect of pH was investigated at pH = 2, 3, 4, 5 and 6 at 25 °C. Decreasing the metal ion removal at low pH may be due to the fact that the competition between $H^+$ and Fe(III) ions for adsorption on the free sites is significant (Fernando et al., 2009). In contrast, with increasing the pH solution, the negative charge increases on the adsorbent surface, which is suitable for the cationic species adsorption (Stafiej and Pyrzynska, 2007; Zhou et al., 2011). Therefore it can be deduced that the sorption of metal cations will be increased with increasing pH, where the metal ionic species become less stable in the studied solution (Chen and Wu, 2004; Yin et al., 2007), and there will be the risk of hydroxide formation and interfering in the adsorption process (Farooq et al., 2010).

### 3.5. Isotherm model determination

One of the most important step in the adsorption process studies is to obtain a reasonable isotherm model of the adsorption process. According to Table 2, the dosage, the contact time and pH were considered as 0.060 (g), 30.0 min, and 5.0, respectively and on the basis of the experimental results the reasonable adsorption isotherms were investigated at optimal conditions at temperatures range of 10.0–50.0 °C. The equilibrium adsorption capacities of Fe (III) ion removing, $q_e$, were calculated from the following equation:

$$q_e = \frac{(C_0 - C_e)}{m} V \tag{4}$$

where $C_0$ and $C_e$ are the initial and equilibrium concentration (mg/L), V (L) is the volume of the sample solution, and m (g) is the mass of the adsorbent. Adsorption isotherm studies were conducted at a concentration range of 10.0 to 20.0 (mg / L) with a dose of 0.060 g (T = 298 K), respectively. The equilibrium adsorption data were analyzed according to the Langmuir (1916) and Freundlich (1906) models. The linear form of these two models are as below respectively (Eqs. (5) and (6)):

$$\frac{1}{q_e} = \left(\frac{1}{K_L q_m}\right)\frac{1}{C_e} + \frac{1}{q_m} \tag{5}$$

$$ln q_e = \left(\frac{1}{n}\right) ln C_e + ln K_F \tag{6}$$

where $C_e$ (mg/L) and $q_e$ (mg/g) are the equilibrium concentration of the adsorbate and the adsorption capacity, respectively. $K_L$ (L/mg) is the Langmuir equilibrium constant and $q_m$ gives the theoretical monolayer saturation capacity or the maximum value of q, $K_F$ ($L^{1/n}mg^{(1-1/n)}/g$) is the Freundlich constant and 1/n is the Freundlich exponent. In the Langmuir adsorption model, the adsorbing surface is smooth and adsorption sites are considered to be equivalent and the adsorption is monolayer. The Freundlich isotherm in general is used for the single-layer or multilayers and is less rigorous for multilayers adsorption. At the same time, in the Freundlich isotherm, a rugged adsorbing surface and adsorption enthalpy are different for each considered location, and at first, the active sites with the higher energy will be occupied. The modified Langmuir isotherm can be also represented in terms of a dimensionless constant or separation factor, $R_L$, which is defined as:

$$R_L = \frac{1}{(1 + K_L C_0)} \tag{7}$$

This factor indicates the type of the studied isotherm that can be irreversible ($R_L = 0$), favorable ($0 < R_L < 1$), linear ($R_L = 1$) or unfavorable ($R_L > 1$) (Mckay et al., 1982). The obtained values of the Langmuir and Freundlich parameters respect to this study are gathered in Table 5 and the considered isotherms are plotted in Fig. 5.

The value of regression coefficient, $R^2$, is an indication for interpreting the isotherm models and experimental results. The more appropriate cases correspond to the conditions for which $R^2$ would be near unity.

## 4. Thermodynamic functions

Thermodynamic study was conducted to find out the thermodynamic nature of the adsorption process. So, the adsorption experiments were carried out at a temperature range of 288 up to 328 (K) with an initial concentration of 15 mg/L of iron (III), 0.060 g of dosage mass at pH = 5.0, and the contact time of 30.0 min. A conditional equilibrium constant, $K_0$, was defined as: $K_0 = q_e/C_e$ at each temperature. So by plotting $ln K_0$ versus 1/T, we can conclude the value of $\Delta H_{ad}^0$ from the slope and $\Delta S_{ad}^0$ from the intercept of the plot respectively (Fig. 5(c)) (Moradi et al., 2010).

$$K_0 = \frac{q_e}{C_e} \tag{8}$$

$$ln K_0 = -\frac{\Delta H_{ad}^0}{R}\left(\frac{1}{T}\right) + \frac{\Delta S_{ad}^0}{R} \tag{9}$$

**Table 5**  The Langmuir and Freundlich isotherm parameters.

| $C_0$ (mg L$^{-1}$) | $q_m$ (mg g$^{-1}$) | Langmuir | | | | Freundlich | | |
| --- | --- | --- | --- | --- | --- | --- | --- | --- |
| | | $K_L$ (L mg$^{-1}$) | $R_L$ | $R^2$ | | n | $K_F$(L$^{0.64}$mg$^{0.36}$g$^{-1}$) | $R^2$ |
| 10.0 | 22.06 | 0.13 | 0.443 | 0.991 | | 1.56 | 3.00 | 0.992 |
| 12.0 | | | 0.443 | | | | | |
| 14.0 | | | 0.398 | | | | | |
| 16.0 | | | 0.329 | | | | | |
| 18.0 | | | 0.307 | | | | | |
| 20.0 | | | 0.283 | | | | | |

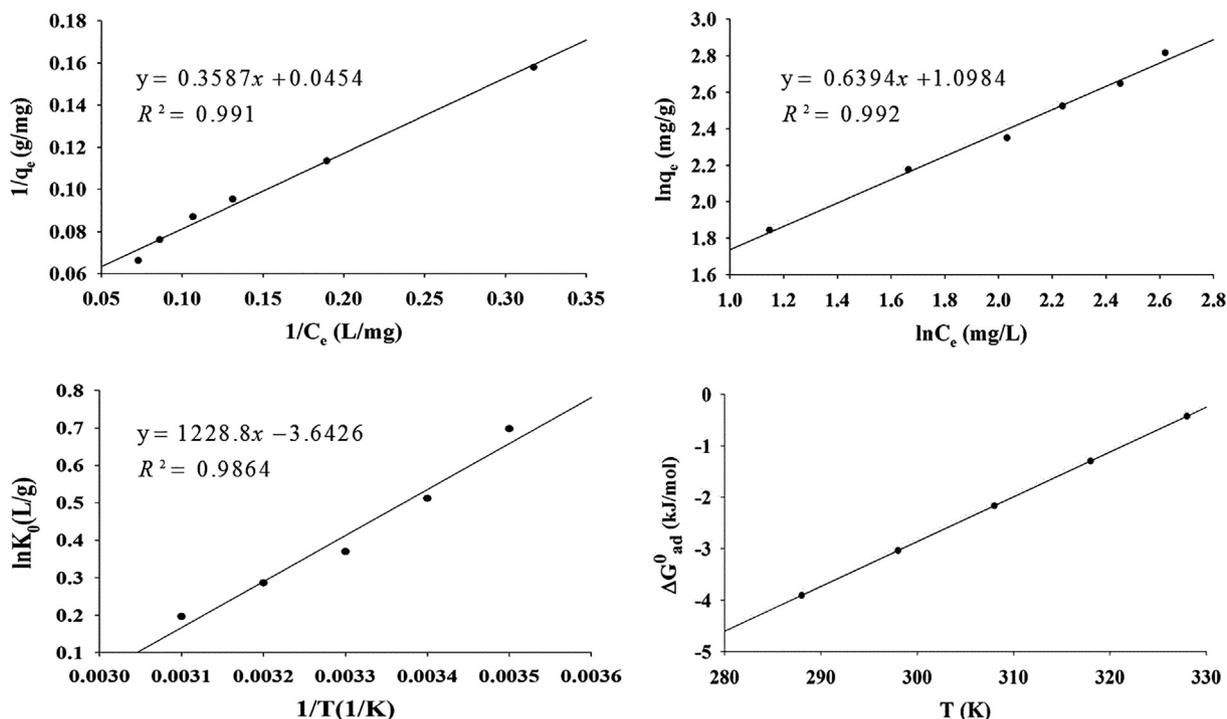**Fig. 5** (a) Langmuir isotherm plot of Fe (III) adsorption (pH 5.0, adsorbent dosage 0.060 g/50 mL, t = 25 °C and contact time 30.0 min), (b) Freundlich isotherm plot of Fe (III) adsorption (pH 5.0, adsorbent dosage 0.060 g/50 mL, t = 25 °C and contact time 30 min), (c) plot of $\ln K_0$ vs, 1/T; pH = 5.0; adsorbent dosage = 0.060 g; contact time = 30.0 min, $C_0$ = 15 mg/L (d) Thermodynamic plot of $\Delta G_{ad}^0$ versus T.

**Table 6**  The values of thermodynamic functions for Fe (III) ion adsorption onto α-Alumina.

| T (K): | 288 | 298 | 308 | 318 | 328 |
|---|---|---|---|---|---|
| $\Delta G^0$ (kJ/mol ) | −3.90 | −3.036 | −2.165 | −1.294 | −0.423 |
| $\Delta H^0$ (kJ/mol ) | – | −28.99 | – | – | – |
| $\Delta S^0$ (J/mol K) | – | −87.1 | – | – | – |

$$\Delta G_{ad}^0 = \Delta H_{ad}^0 - T\Delta S_{ad}^0 \qquad (10)$$

$$\Delta G_{ad}^0 = -RT \ln K_0 \qquad (11)$$

It is worthwhile to pay attention to the $\Delta G_{ad}^0$ trend respect to the temperature. Regarding Eq. (10) and the negative values of $\Delta H_{ad}^0$ and $\Delta S^0$ad, it is easy to conclude that, $\Delta G_{ad}^0$ will be algebraically increased with increasing temperature (Fig. 5 (d)). In turn, the standard Gibbs free energy change, $\Delta G_{ad}^0$, was also calculated at each temperature from Eq. (10). The resulted thermodynamic functions of the studied adsorption process at 25 °C are listed in Table 6.

## 5. Conclusion

Characterization of the synthesized α-Alumina powder showed that it has a good capacity for Fe (III) ion removal from the aqueous media. Using this synthesized adsorbent, various adsorption experiments for removing Fe (III) ions from the considered solution phases were done in the various conditions. The design of the response method was used to corpo-

rate the experimental results for predicting the optimum conditions for achieving to the optimum adsorption percentage. This method showed that the adsorption percentage of Fe (III) ions onto the synthesized α-Alumina maybe reaches up to %68. In addition, the effect of the various variables such as: initial concentration, pH and so on were studied, we concluded that the effect of pH on the adsorption percent was dominant, while the other variables were less effective. The adsorption experimental results were examined with the Langmuir and Freundlich isotherm models. These two models were capable to represent the experimental data, but the Freundlich model fitted better our results. Thermodynamic study of the adsorption process showed that the intended process at the experimental conditions, is exothermic ($\Delta H_{ad}^0$ < 0) and spontaneous or exergonic ($\Delta G_{ad}^0$ < 0) and with a decrease in the randomness ($\Delta S_{ad}^0$ < 0). Based on the $\Delta H_{ad}^0$ value, it maybe to conclude that the studied adsorption is a physisorption one, so the weak attractive forces acting between the sorbent and the sorbate are responsible for occurring the studied adsorption. The entropy decrease is almost due to the Fe (III) ions depositing onto the adsorbent surface.

## Declaration of Competing Interest

The authors declared that there is no conflict of interest.

## Acknowledgement

## References

Al'myasheva, O.V. et al, 2005. Preparation of nanocrystalline alumina under hydrothermal conditions. Inorg. Mater. 41 (5), 460–467.

Amuda, O.S., Giwa, A.A., Bello, I.A., 2007. Removal of heavy metal from industrial wastewater using modified activated coconut shell carbon. Biochem. Eng. J. 36, 174–181.

Bodaghi, M. et al, 2009. Synthesis and characterization of nanocrystalline a-$Al_2O_3$ using Al and $Fe_2O_3$ (hematite) through mechanical alloying. Solid State Sci. 11, 496–500.

Chen, J.P., Wu, S., 2004. Acid/base-treated activated carbons: characterization of functional groups and metal adsorptive properties. Langmuir 20 (6), 2233–2242.

Deady, E. et al, 2016b. A review of the potential for rare-earth element resources from European red muds: examples from Seydisehir, Turkey and Parnassus-Giona, Greece, Mineral. Mineralog. Mag. 80, 43–61.

Deady, É.A. et al, 2016a. A review of the potential for rare-earth element resources from European red muds: examples from Seydişehir, Turkey and Parnassus-Giona, Greece. Mineral. Mag. 80 (1), 43–61.

Edrissi, M., Norouzbeigi, R., 2007. Synthesis and characterization of alumina nanopowders by combustion of nitrate-amino acid gels. Mater. Sci.-Poland 25 (4), 1029–1040.

Farooq, U. et al, 2010. Biosorption of heavy metal ions using wheat based biosorbents–a review of the recent literature. Bioresour Technol. 101, 5043–5053.

Fernando, A. et al, 2009. Production of biosorbents from waste olive cake and its adsorption characteristics for $Zn^{2+}$ ion. Sustainability 1, 277–297.

Freundlich, H.M.F., 1906. Uber die adsorption in losungen. Z Phys. Chem. 57 (A), 385–470.

He, T., He, Q., Wang, N., 2005. Synthesis of nano-sized YSZ powders from glycine-nitrate process and optimization of their properties. J. Alloy. Compd. 396 (1–2), 309–315.

Jadhav, U.U., Hocheng, H., 2012. A review of recovery of metals from industrial waste. J. Achiev. Mater. Manuf. Eng. 54 (2), 159–167.

Klauber, C., Gräfe, M., Power, G., 2011. Bauxite residue issues: II. Options for residue utilization. Hydrometallurgy 108 (1–2), 11–32.

Kumar, S., Kumar, R., Bandopadhyay, A., 2006. Innovative methodologies for the utilisation of wastes from metallurgical and allied industries. Resour. Conserv. Recycl. 48 (4), 301–314.

Langmuir, I., 1916. The constitution and fundamental properties of solids and liquids. J. Am. Chem. Soc. 38 (11), 2221–2295.

Lide, D.R., 2004. In: CRC handbook of chemistry and physics, vol. 85. CRC Press.

Liu, Y., Naidu, R., 2014. Hidden values in bauxite residue (red mud): recovery of metals. Waste Manage. 34 (12), 2662–2673.

Mckay, G.B.H.S., Blair, H.S., Gardner, J.R., 1982. Adsorption of dyes on chitin. J. Appl. Polym. Sci. 27 (8), 3043–3057.

Montgomery, D.C., 2012. Desiggn and Analysis of Experiment. John Wiley & Sons.

Moradi, O. et al, 2010. The studies of equilibrium and thermodynamic adsorption of Pb(II), Cd(II) and Cu(II) ions from aqueous solution onto SWCNTs and SWCNT-COOH surfaces. Fullerenes, Nanotubes, Carbon Nanostruct. 18 (3), 285–302.

Pati, R.K., Ray, J.C., Pramanik, P., 2000. A novel chemical route for the synthesis of nanocrystalline a-Al O powder. Mater. Lett. 44, 299–303.

Piticescu, R. et al, 2001. Hydrothermal synthesis of zirconia nanomaterials. J. Eur. Ceram. Soc. 21 (10–11), 2057–2060.

Rahmani, A., Mousavi, H.Z., Fazli, M., 2010. Effect of nanostructure alumina on adsorption of heavy metals. Desalination 253, 94–100.

Segurola, J. et al, 1999. Design of eutectic photoinitiator blends for UV/visible curable acrylated printing inks and coatings. Prog. Org. Coat. 37 (1–2), 23–37.

Stafiej, A., Pyrzynska, K., 2007. Adsorption of heavy metal ions with carbon nanotubes. Sep. Purif. Technol. 58 (1), 49–52.

Wang, K.Q. et al, 2010. Experimental investigation on leaching scandium from red mud by hydrochloric acid. Chinese Rare Earths 1, 95–98.

Wasserstein, R.L., Lazar, N.A., 2016. The ASA's statement on p-values: context, process, and purpose. Am. Stat. 70 (2), 129–133.

Wen, Hui-Ling et al, 1999. Size characterization of θ-and α-$Al_2O_3$ crystallites during phase transformation. Nanostruct. Mater. 11 (1), 89–101.

Yin, C.Y., Aroua, M.K., Daud, W.M.A.W., 2007. Review of modifications of activated carbon for enhancing contaminant uptakes from aqueous solutions. Sep. Purif. Technol. 52 (3), 403–415.

Zhou, X., Xue, X., Jiang, W., 2011. Study on adsorption of heavy metal ion in metallurgical wastewater by sepiolite. In: 2nd International Conference on Environmental Science and Development IPCBEE. IACSIT Press, Singapore, pp. 100–103.